Article ID: 1000-324X(2022)05-0561-06 **DOI:** 10.15541/jim20210271

Preparation of Epitaxial Metallic $LaNiO_3$ Thin Film by Polymer Assisted Deposition

YANG Zhu[1,2], GUO Shaobo[1], CAI Henghui[1,2], DONG Xianlin[1,2,3], WANG Genshui[1,2,3]

(1. Key Laboratory of Inorganic Functional Materials and Devices, Shanghai Institute of Ceramics, Chinese Academy of Sciences, Shanghai 200050, China; 2. Center of Materials Science and Optoelectronics Engineering, University of Chinese Academy of Sciences, Beijing 100049, China; 3. State Key Laboratory of High Performance Ceramics and Superfine Microstructure, Shanghai Institute of Ceramics, Chinese Academy of Sciences, Shanghai 200050, China)

Abstract: $LaNiO_3$ (LNO), as a promising material in ferroelectric super lattices, super conductive heterostructures and catalysts has recently attracted great interest. Herein, a facile and low-cost polymer assisted deposition (PAD) method is established to prepare epitaxial LNO thin films on (001) orientated $SrTiO_3$ (STO) with excellent conductivity. Various structural and electrical characterizations of the film were investigated. The film has good crystallinity with a full-width at half-maximum value of 0.38° from the rocking curve for the (002) reflection. High resolution XRD φ-scans further confirmed the heteroepitaxial growth of LNO film on STO substrate. There are four peaks separated by 90°, showing that the LNO thin film is cubic-on-cubic grown on STO substrate. *In-situ* high temperature XRD measurement showed epitaxial growth of LNO thin film on STO substrate. Metal cations could be released orderly on the monocrystalline substrate and epitaxial crystallization occurs after decomposition of polymer. XPS results indicated that $LaNiO_3$ thin film fabricated by PAD was stoichiometric without oxygen vacancy. The atomic force microscopy analysis showed that the smooth surface with root-mean-square surface roughness was 0.67 nm. The resistivity as functions of temperature revealed that it has good conductivity from 10 K to 300 K. All results demonstrate that the $LaNiO_3$ thin films deposited by PAD have better comprehensive performance, indicating that PAD method has great potential for preparing epitaxial functional thin film materials.

Key words: $LaNiO_3$; conductive film; polymer assisted deposition; epitaxial

$LaNiO_3$ (LNO) has attracted much attention in recent years not only due to its metallic property at all temperatures among rare earth nickelate, but also owing to its alternative to Pt to serve as bottom electrode of ferroelectric thin film capacitors[1-2]. LNO has the perovskite structure with a pseudo-cubic lattice parameter of 0.384 nm[3]. It has been reported that the use of LNO bottom electrode can improve the performance of the ferroelectric thin film device such as fatigue characteristics and leakage current characteristics due to the mutual diffusion between Pt electrode and ferroelectric thin film[4-5]. At the same time, the orientation of LNO seed layer can induce the oriented growth of ferroelectric thin films[6]. And the epitaxial strain has been proved to enhance the remanent polarization and increase the Curie temperature in ferroelectric epitaxy[7-8].

Synthesis of LNO thin films have been reported by a variety of techniques including physical vapor deposition (radio frequency magnetron sputtering (RF-MS)[9], pulsed laser deposition (PLD)[10], molecular beam epitaxy (MBE)[11]) and chemical solution deposition (CSD)[12]. High-quality epitaxial films can be obtained by physical vapor deposition, but these processes are associated with expensive and complex equipment, vacuum environment, limited deposition area and high costs[13]. While in the traditional CSD process, metallic organic precursors with high activity are used as reaction sources to generate various oligomers through hydrolysis. These oligomers,

Received date: 2021-04-26; **Revised date:** 2021-05-23; **Published online:** 2021-07-20
Foundation item: National Natural Science Foundation of China (11774366); International Partnership Program of Chinese Academy of Sciences (GJHZ1821)
Biography: YANG Zhu (1996–), male, Master candidate. E-mail: yangzhu@student.sic.ac.cn
杨 柱(1996–), 男, 硕士研究生. E-mail: yangzhu@student.sic.ac.cn
Corresponding author: WANG Genshui, professor. E-mail: genshuiwang@mail.sic.ac.cn;
GUO Shaobo, senior engineer. E-mail: guoshaobo@ mail.sic.ac.cn
王根水, 研究员. E-mail: genshuiwang@mail.sic.ac.cn; 郭少波, 高级工程师. E-mail: guoshaobo@mail.sic.ac.cn

which contain metal ions, with the proper viscosity, are easy to rotate and uniformly coating, and can be made into ceramic materials by combustion of organic matter at high temperatures[14]. Although this method needs simple equipment and low cost, it cannot meet the requirements of the epitaxial growth of thin films. Moreover, many functional compound materials cannot be deposited because many metal precursors react violently with water to form metal hydroxides and precipitate out of the solution even before coating the solution on the substrates. The degree of hydrolysis can be in question owing to the differences in chemical reactivity among the metals used in the solution[15]. Thus, it is necessary to find a synthetic method which can prepare epitaxial films like the physical method while having the advantages of the chemical method.

Polymer assisted deposition is a new chemical solution method developed in 2004[16]. This technique has been widely used for the epitaxial growth of thin films in different fields such as oxides[17], nitrides[18], carbides[19], *etc*[20]. The key to the successful of epitaxial growth of thin films is the use of polyethyleneimine (PEI) with functional $-NH_2$ groups to bind metal that serves both to coordinate, stabilize cations and maintain an even distribution of the metal cations in solution[21-22]. PEI can not only encapsulate the metal to prevent chemical reaction, but also control the viscosity of the precursor by adjusting the molecular weight of PEI[23]. Therefore, the solution has adequate viscosity to coat on the substrate evenly. After the decomposition of PEI, metal cations can be released orderly on the monocrystalline substrate and epitaxial crystallization occurs[16]. Compared with the physical vapor deposition, PAD requires no vacuum, which has the advantages of simple operation, simple equipment and low cost. Compared with the Sol-Gel method, PAD avoids the hydrolysis and condensation reaction of precursors, so it is easier to obtain stable precursors with precise stoichiometric ratio. The PAD method offers several advantages over CSD method, such as epitaxial growth, no need of ageing and easy control of viscosity.

This study presents a new attempt to prepare LNO epitaxial film by PAD. Various analyses on the structure and chemical composition of the conductive LNO thin film were carried out. It is proved that the crystallization occurs at crystallization temperature after the decomposition of PEI which results in the epitaxial growth of LNO thin film.

1 Experimental

Epitaxial LNO thin films were fabricated on (001) oriented $SrTiO_3$ (STO) single-crystal substrate by PAD. The precursor for the growth of LNO film was obtained by the following steps. Lanthanum acetate hydrate ($La(NO_3)_3\cdot 6H_2O$, 99.99%, Aladdin Industrial Medicines Co.Ltd) and nickel nitrate hexahydrate ($Ni(NO_3)_2\cdot 6H_2O$, 98%, China National Industrial Medicines Co.Ltd) as sources of metal were dissolved in deionized H_2O. Both polyethyleneimine (PEI, 50% (in mass) in H_2O, Aladdin Industrial Medicines Co.Ltd) and ethylenediaminetetraacetic acid (EDTA, 99%, Aladdin Industrial Medicines Co.Ltd) were used to complex the metal cations. In detail, EDTA was 1∶1 molar ratio with metal ion, and PEI was incorporated into the solution in a 1:1 mass ratio with EDTA. After stirring for 24 h, a transparent blue solution with reasonable viscosity was achieved. The solution concentration was 0.15 mol/L. The precursor solution was spin-coated onto STO (001) substrate at 5000 r/min for 30 s to obtain LNO wet film. The wet film was heated at 700 ℃ for 30 min in air to form a dense film.

Crystallinity of the film and the heteroepitaxial relationships between the film and the substrate were measured by high resolution X-ray diffractometer (HRXRD, D8 Discover, Bruker, Germany). Atomic force microscope (AFM, FM-Nanoview6800, FSM-Precision, China) was used to characterize surface roughness of the film. The thickness and lattice parameter of the film were characterized by the high-resolution transmission electron microscopy (HRTEM, JEM-2100F, JEOL, Japan). Chemical composition of films and oxidation state of elements were detected by X-ray photoelectron spectroscope (XPS, ESCAlab-250, Thermo Fisher, England). The resistivity of the LNO film was performed from 10 K to 300 K using a four-probe technique by a physical property measurement system (PPMS, PPMS-9T, Quantum Design, USA).

2 Results and discussion

Fig. 1(a) presents the θ-2θ scan of LNO film on STO (001). It is obvious that only (001) peak of the film and substrate can be seen, indicating that the LNO film exhibits substrate orientation. The calculated lattice parameter obtained from the position of (002) reflection is 0.3838 nm, which is well consistent with the theoretical value 0.384 nm[3]. Fig. 1(b) shows the rocking-curve of the (002) peak. A full width at half-maximum (FWHM) value is 0.38°, suggesting that the LNO film fabricated by PAD has good crystallization quality. Additionally, to further confirm the heteroepitaxial growth of LNO film on STO substrate, XRD φ-scans of reflections of LNO (202) and STO (202) (Fig. 1(c)) were carried out. It can be seen from the φ-scans that there are four peaks

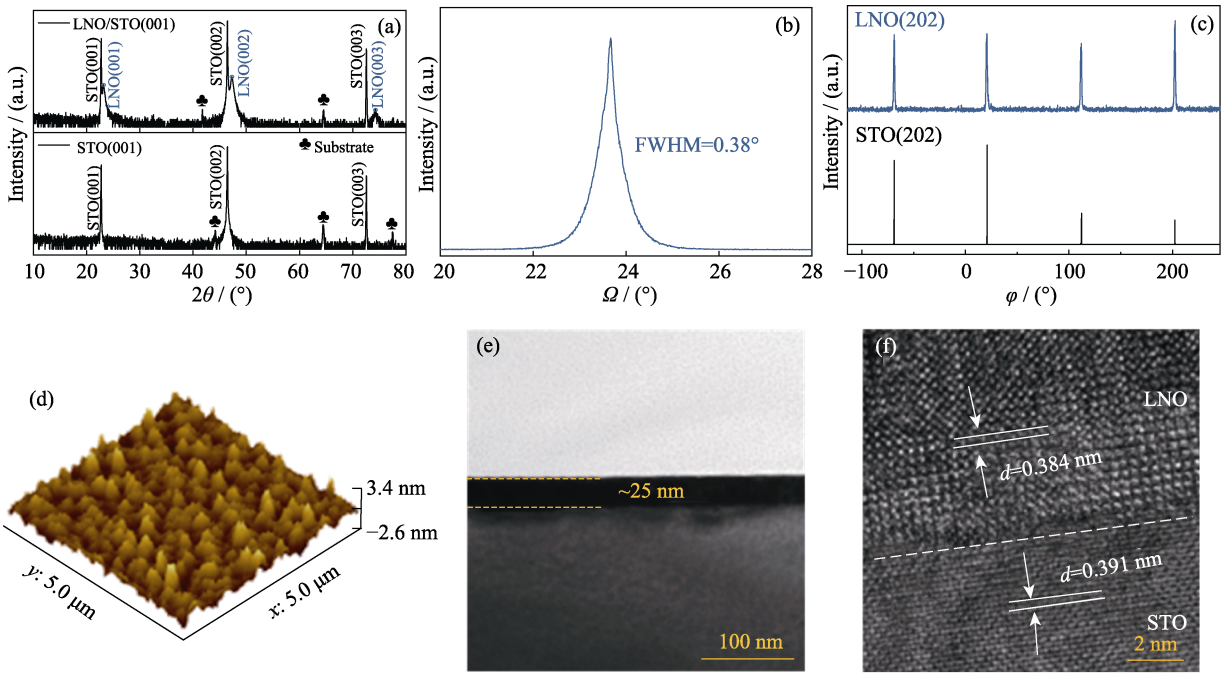

Fig. 1　Charaterization of as-prepared LNO film

(a) HRXRD patterns of the LNO films; (b) Rocking-curve of the (002) LNO reflection; (c) φ-scans from (202) reflection of LNO and (202) of STO; (d) 3D AFM micrograph of LNO film; (e) Bright-field cross-sectional TEM image of LNO film on STO substrate; (f) Cross-sectional HRTEM image of the interface between LNO and STO

separated by 90°, showing that the LNO thin film is cubic-on-cubic grown on STO substrate. The heteroepitaxial relationships between the LNO film and the STO substrate can be described as (001)LNO||(001)STO and [101]LNO||[101]STO. As shown in Fig. 1(d), the RMS roughness of LNO film is 0.67 nm, indicating that the surface is smooth. Fig. 1(e) shows the cross-sectional HRTEM image of LNO film on STO substrate. And the thickness of the film can be measured as ~25 nm. The detailed epitaxial interface structure between the LNO thin film and the STO substrate through the HRTEM is exhibited in Fig. 1(f). The excellent epitaxial growth could be attributed to the relatively small lattice mismatch ~1.7% between the film (a_{LNO}=0.384 nm measured through the (001) lattice plane spacing) and the substrate (a_{STO}=0.391 nm).

To show the epitaxial growth of LNO thin film on STO substrate, the wet film coated by LNO precursor was tested by *in-situ* high temperature XRD measurement. It can be seen from Fig. 2 that there is no obvious change in the XRD pattern in the low temperature zone. With the increase of the temperature up to 500 ℃, PEI gradually decomposes and at the end of the pyrolysis there are no other peaks observed except for the substrate. Until the beginning of the crystallization at 700 ℃, the (002) orientation peak of LNO film appears. In other words, crystallization of the film occurs after the decomposition temperature of the PEI polymer. The

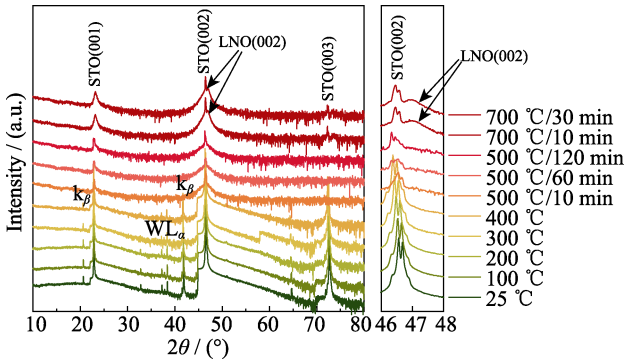

Fig. 2　*In-situ* XRD patterns of LNO film on STO substrate at different temperatures

complete degradation of PEI is above 550 ℃ by Thermogravimetric Analysis[22]. That means that the high decomposition temperature of PEI prevents the formation of the film below this temperature which is basically consistent with the above *in-situ* XRD results. After the decomposition of PEI, metal cations can be released orderly on the monocrystalline substrate and epitaxial crystallization occurs.

Fig. 3 shows the XPS survey spectrum and La3d, Ni2p and O1s spectra for the film fabricated by PAD. It can be seen from Fig. 3(a) that only the peak of La, Ni, O and C elements can be found in the survey spectrum. Except for the surface adsorbed carbon, there is no detectable impurity elements. Fig. 3(b) gives the XPS spectrum of La with high resolution which presents the binding energy

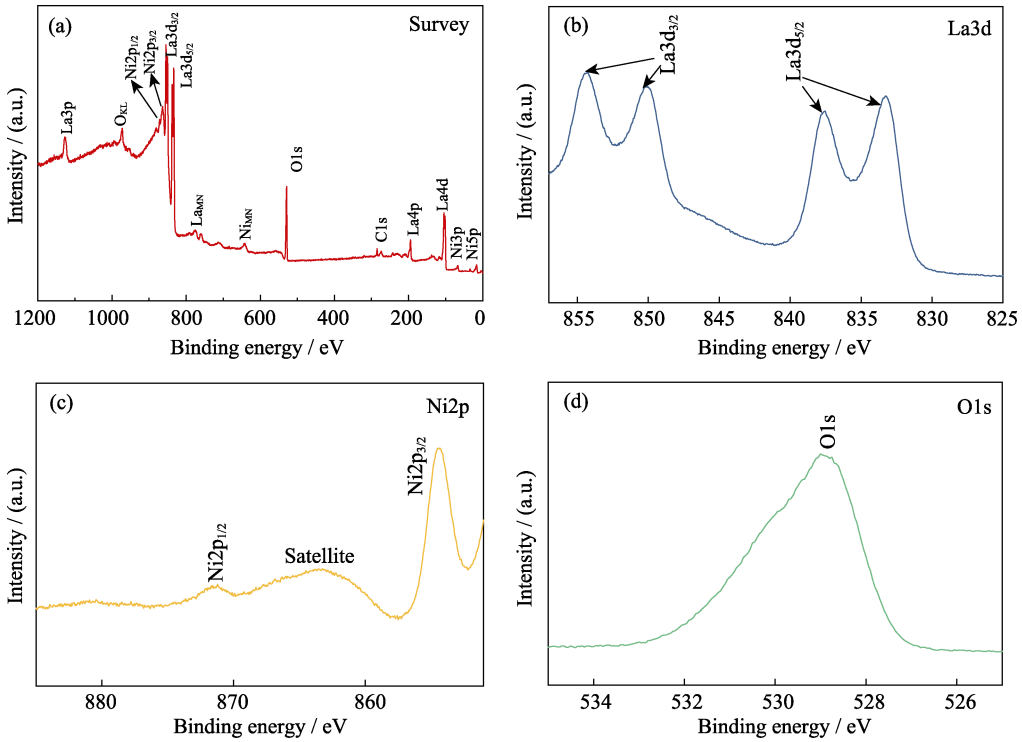

Fig. 3 Survey (a), La3d (b), Ni2p (c) and O1s (d) XPS spectra of $LaNiO_3$

of $La3d_{3/2}$ between 854.3 and 850.1 eV and $La3d_{5/2}$ between 837.5 and 833.2 eV (standard value: $La3d_{3/2}$~853.0 eV; $La3d_{5/2}$~836.0 eV)[24-25]. Fig. 3(c) represents the narrow scan of Ni2p. The $Ni2p_{3/2}$ spin-orbit is located at 854.4 eV accompanied by a satellite peak locating at higher binding energy of 863.4 eV. The chemical valence state of Ni ion can be judged from $Ni2p_{1/2}$ bonding energy peak[26-27]. The $Ni2p_{1/2}$ usually has a single peak for Ni^{3+}, while a double peak for Ni^{2+}. Additionally, the existence of Ni^{2+} degenerates the conductive properties of LNO films. In Fig. 3(c), the $Ni2p_{1/2}$ spin-orbit with a single peak at 871.7 eV was observed. It can be inferred that the oxidation state of nickel ion in the LNO film prepared by PAD is +3, which is consistent well with the good conductive property described as follows. Fig. 3(d) shows the narrow scan of O1s. The only peak at binding energy of 528.9 eV is considered to be the lattice oxygen in LNO. This indicates that LNO thin film annealed in air do not have oxygen vacancies which means that $LaNiO_3$ fabricated by PAD is stoichiometric.

Fig. 4 shows the resistivity from 10 to 300 K of the LNO film on STO substrate with a thickness of 25 nm. The LNO film measured by a standard four-probe method presents metallic resistivity *versus* temperature behavior which means that the resistivity increases by increasing temperature. The LNO thin film has a room temperature resistivity of 160 μΩ·cm. Table 1 summarizes the room-temperature resistivity of LNO thin films deposited by different methods on single crystal substrate.

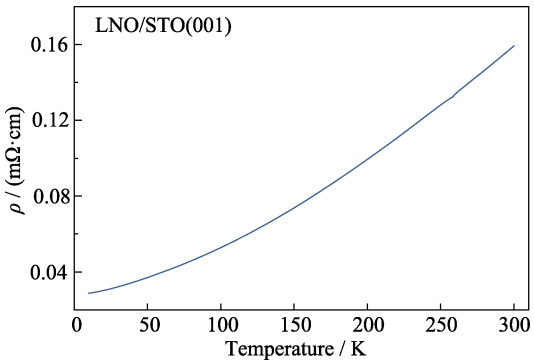

Fig. 4 Temperature dependence of resistivity of 25 nm LNO film on STO substrate

Table 1 Summary of the parameters of LNO films grown by different methods

Method	Substrate	Orientation	*d*/nm	$\rho_{300\ K}$/(μΩ·cm)	Ref.
SCD	$SrTiO_3$	Preferred orientation	100	340	[31]
RF-MS	$LaAlO_3$	Epitaxial	9	~150	[28]
MBE	$SrTiO_3$	Epitaxial	36	~90	[29]
PLD	$SrTiO_3$	Epitaxial	50–60	100	[30]
PAD	$SrTiO_3$	Epitaxial	25	160	This work

It should be noted that the LNO thin film deposited by PAD is epitaxial growth as compared with chemical solution deposition, and has a low resistivity comparable to that fabricated by physical vapor deposition[28-30].

3 Conclusion

In summary, we have successfully fabricated epitaxial $LaNiO_3$ thin film on $SrTiO_3$ substrate through polymer assisted deposition. XRD and HRTEM results reveal that the film has good crystallinity and epitaxial quality. Additionally, the *in-situ* XRD measurement has been carried out to elucidate the epitaxial growth process of LNO thin film. The resistivity result shows all metallic property with good conductive property from 10 to 300 K. The successful growth of the LNO thin film provides a new approach in preparing epitaxial functional thin film material by using low-cost PAD.

Reference:

[1] PONTES D S L, PONTES F M, CHIQUITO A J, *et al*. Investigation of the structural, optical and dielectric properties of highly (100)-oriented $(Pb_{0.60}Ca_{0.20}Sr_{0.20})TiO_3$ thin films on $LaNiO_3$ bottom electrode. *Materials Science and Engineering: B*, 2014, **185:** 123–128.

[2] PONTES D S L, CAPELI R A, GARZIM M L, *et al*. Structural, microstructural, optical and electrical properties of (Pb,Ba,Sr)TiO_3 films growth on conductive $LaNiO_3$-coated $LaAO_3$(100) and Pt/Ti/SiO_2/Si substrates. *Materials Letters*, 2014, **121:** 93–96.

[3] ZHU J, ZHENG L, ZHANG Y, *et al*. Fabrication of epitaxial conductive $LaNiO_3$ films on different substrates by pulsed laser ablation. *Materials Chemistry and Physics*, 2006, **100(2/3):** 451–456.

[4] CHEN M S, WU T B, WU J M. Effect of textured $LaNiO_3$ electrode on the fatigue improvement of $Pb(Zr_{0.53}Ti_{0.47})O_3$ thin films. *Applied Physics Letters*, 1996, **68(10):** 1430–1432.

[5] CHAE B G, YANG Y S, LEE S H, *et al*. Comparative analysis for the crystalline and ferroelectric properties of Pb(Zr,Ti)O_3 thin films deposited on metallic $LaNiO_3$ and Pt electrodes. *Thin Solid Films*, 2002, **410(1/2):** 107–113.

[6] LI W L, ZHANG T D, XU D, *et al*. $LaNiO_3$ seed layer induced enhancement of piezoelectric properties in (100)-oriented (1–*x*)BZT-*x*BCT thin films. *Journal of the European Ceramic Society*, 2015, **35(7):** 2041–2049.

[7] WANG J, NEATON J B, ZHENG H, *et al*. Epitaxial $BiFeO_3$ multiferroic thin film heterostructures. *Science*, 2003, **299(5613):** 1719–1722.

[8] LEE J H, MURUGAVEL P, RYU H, *et al*. Epitaxial stabilization of a new multiferroic hexagonal phase of $TbMnO_3$ thin films. *Advanced Materials*, 2006, **18(23):** 3125–3129.

[9] SCHERWITZL R, GARIGLIO S, GABAY M, *et al*. Metal-insulator transition in ultrathin $LaNiO_3$ films. *Physical Review Letters*, 2011, **106(24):** 246403.

[10] LIU P, NING X. Anisotropy of core-level spectra and the correlation with transport properties of epitaxial lanthanum nickel oxide thin films. *Physica B: Condensed Matter*, 2020, **589:** 412199.

[11] CHEN P, XU S Y, ZHOU W Z, *et al*. *In situ* reflection high-energy electron diffraction observation of epitaxial $LaNiO_3$ thin films. *Journal of Applied Physics*, 1999, **85(5):** 3000–3002.

[12] MAMBRINI G P, LEITE E R, ESCOTE M T, *et al*. Structural, microstructural, and transport properties of highly oriented $LaNiO_3$ thin films deposited on $SrTiO_3$ (100) single crystal. *Journal of Applied Physics*, 2007, **102(4):** 043708.

[13] CHO C R, PAYNE D A, CHO S L. Solution deposition and heteroepitaxial crystallization of $LaNiO_3$ electrodes for integrated ferroelectric devices. *Applied Physics Letters*, 1997, **71(20):** 3013–3015.

[14] FEI L, NAEEMI M, ZOU G, *et al*. Chemical solution deposition of epitaxial metal-oxide nanocomposite thin films. *Chemical Record*, 2013, **13(1):** 85–101.

[15] GOH P C, YAO K, CHEN Z. Reaction mechanisms of ethylenediaminetetraacetic acid and diethanolamine in the precursor solution for producing (K, Na)NbO_3 thin films with outstanding piezoelectric properties. *The Journal of Physical Chemistry C*, 2012, **116(29):** 15550–15556.

[16] JIA Q X, MCCLESKEY T M, BURRELL A K, *et al*. Polymer-assisted deposition of metal-oxide films. *Nature Materials*, 2004, **3(8):** 529–532.

[17] LIN Y, LEE J S, WANG H, *et al*. Structural and dielectric properties of epitaxial $Ba_{1-x}Sr_xTiO_3$ films grown on $LaAlO_3$ substrates by polymer-assisted deposition. *Applied Physics Letters*, 2004, **85(21):** 5007–5009.

[18] LUO H M, WANG H Y, BI Z X, *et al*. Epitaxial ternary nitride thin films prepared by a chemical solution method. *Journal of the American Chemical Society*, 2008, **130(46):** 15224–15225.

[19] ZOU G, LUO H, ZHANG Y, *et al*. A chemical solution approach for superconducting and hard epitaxial NbC film. *Chemical Communications*, 2010, **46(41):** 7837–7839.

[20] KUMAH D P, NGAI J H, KORNBLUM L. Epitaxial oxides on semiconductors: from fundamentals to new devices. *Advanced Functional Materials*, 2019, **30(18):** 1901597.

[21] BURRELL A K, MARK MCCLESKEY T, JIA Q X. Polymer assisted deposition. *Chemical Communications*, 2008, **11(11):** 1271–1277.

[22] VILA-FUNGUEIRIÑO J M, RIVAS-MURIAS B, RUBIO-ZUAZO J, *et al*. Polymer assisted deposition of epitaxial oxide thin films. *Journal of Materials Chemistry C*, 2018, **6(15):** 3834–3844.

[23] WANG H, FRONTERA C, HERRERO-MARTIN J, *et al*. Aqueous chemical solution deposition of functional double perovskite epitaxial thin films. *Chemistry*, 2020, **26(42):** 9338–9347.

[24] YANG E H, MOON D J. Synthesis of $LaNiO_3$ perovskite using an EDTA-cellulose method and comparison with the conventional pechini method: application to steam CO_2 reforming of methane. *RSC Advances*, 2016, **6(114):** 112885–112898.

[25] WANG G, LING Y, LU X, *et al*. A mechanistic study into the catalytic effect of $Ni(OH)_2$ on hematite for photoelectrochemical water oxidation. *Nanoscale*, 2013, **5(10):** 4129–4133.

[26] TSUBOUCHI K, OHKUBO I, KUMIGASHIRA H, *et al*. Epitaxial growth and surface metallic nature of $LaNiO_3$ thin films. *Applied Physics Letters*, 2008, **92(26):** 262109.

[27] HE B,WANG Z. Effect of substrate temperature on microstructure and electrical properties of $LaNiO_3$ films grown on SiO_2/Si substrates by pulsed laser deposition under a high oxygen pressure. *Applied Physics A*, 2016, **122(10):** 905.

[28] SON J, MOETAKEF P, LEBEAU J M, *et al*. Low-dimensional mott material: transport in ultrathin epitaxial $LaNiO_3$ films. *Applied Physics Letters*, 2010, **96(6):** 062114.

[29] DOBIN A Y, NIKOLAEV K R, KRIVOROTOV I N, *et al*. Electronic and crystal structure of fully strained $LaNiO_3$ films. *Physical Review B*, 2003, **68(11):** 113408.

[30] ZHU M, KOMISSINSKIY P, RADETINAC A, *et al*. Effect of composition and strain on the electrical properties of $LaNiO_3$ thin films. *Applied Physics Letters*, 2013, **103(14):** 141902.

[31] MIYAKE S, FUJIHARA S, KIMURA T. Characteristics of oriented $LaNiO_3$ thin films fabricated by the Sol-Gel method. *Journal of the European Ceramic Society*, 2001, **21(10/11):** 1525–1528.

高分子辅助沉积法制备 $LaNiO_3$ 外延导电薄膜

杨 柱[1,2], 郭少波[1], 蔡恒辉[1,2], 董显林[1,2,3], 王根水[1,2,3]

(1. 中国科学院 上海硅酸盐研究所, 无机功能材料与器件实验室, 上海 200050; 2. 中国科学院大学 材料科学与光电子工程中心, 北京 100049; 3. 中国科学院 上海硅酸盐研究所, 高性能陶瓷和超微结构国家重点实验室, 上海 200050)

摘 要: 近年来 $LaNiO_3$(LNO)作为铁电超晶格、超导异质结和催化剂材料引起了广泛关注。本研究采用简便、低成本的高分子辅助沉积法(Polymer Assisted Deposition, PAD), 在(001)取向的 $SrTiO_3$(STO)单晶衬底上制备了导电性能优异的 LNO 外延薄膜, 并对其进行各种结构和电学表征。摇摆曲线半高宽为 0.38°, 表明 LNO 薄膜结晶度良好。高分辨 XRD 的 φ 扫描进一步证实 LNO 薄膜在 STO 衬底上异质外延生长。原位变温 XRD 测试进一步表征了 LNO 薄膜的外延生长过程。结果表明, 聚合物分解之后金属阳离子在单晶基体上有序释放并外延结晶。XPS 结果表明, 采用 PAD 制备的 $LaNiO_3$ 薄膜不存在氧空位。薄膜表面光滑, 粗糙度为 0.67 nm。在 10~300 K 温度区间内的变温电阻率表明 LNO 薄膜具有良好的导电性能。上述结果表明：PAD 制备的 $LaNiO_3$ 薄膜具有较好的综合性能, PAD 在制备外延功能薄膜材料方面具有很大的潜力。

关 键 词: $LaNiO_3$; 导电薄膜; 高分子辅助沉积法; 外延

中图分类号: TQ174 **文献标志码**: A